Journal of Nuclear Materials 396 (2010) 202–207

Contents lists available at ScienceDirect

Journal of Nuclear Materials

journal homepage: www.elsevier.com/locate/jnucmat

Thermal conductivity of SiC after heavy ions irradiation

J. Cabrero [a,b,*], F. Audubert [b], R. Pailler [a], A. Kusiak [c], J.L. Battaglia [c], P. Weisbecker [a]

[a] LCTS, University of Bordeaux, 3 allée de la Boétie, 33600 Pessac, France
[b] CEA, DEN/DEC/SPUA, Cadarache, 13108 Saint Paul lez Durance, France
[c] Laboratory Transferts Ecoulements Fluides Energétique, University of Bordeaux, 351 cours de la libération, 33405 Talence Cedex, France

ARTICLE INFO

Article history:
Received 3 July 2009
Accepted 10 November 2009

ABSTRACT

In this study, we performed irradiation experiments on α-SiC samples, with heavy ions at room temperature (74 MeV Kr, fluence of 5×10^{14} ions cm^{-2}). This energy results in an irradiated layer of about 9.6 μm for SiC. TEM and Raman analyses reveal a graded damaged material. In the electronic interactions domain SiC is weakly damaged whereas it becomes fully amorphous in the nuclear interactions domain. According to the structural examinations, the irradiated SiC is considered as a multilayered material. Thermal conductivity in both electronic and nuclear interactions domains is measured as a function of temperature and annealing temperature. It appears that such an approach is reliable to estimate thermal conductivity of ceramics under neutron irradiation.

© 2009 Published by Elsevier B.V.

1. Introduction

Silicon carbide presents interesting features with respect to high temperature applications in neutron radiation environment [1]. Simulation of neutron damage using ions has been considered as a prominent alternative due to the limitations and difficulties generally encountered with neutron irradiation. The main irradiation damage in a nuclear core of inert materials such as silicon carbide is primarily due to atomic displacement by fast neutrons. Such damages are roughly simulated from irradiation with heavy ions. Extensive studies were carried out on microstructure [2,3], amorphisation and recrystallization [4–7] and thermal conductivity [8–10] of ion irradiated SiC. The present work is devoted to the thermal conductivity measurement of 74 MeV Kr irradiated SiC as a function of temperature while the structural evolution of the irradiated samples is investigated by Raman Micro Spectroscopy (MRS) and Transmission Electron Microscopy (TEM).

2. Experimental

Commercial silicon carbide (α-SiC, grain size ≈ 5 μm, porosity ≈ 4%, sintering aids: B_4C), is the investigated ceramic. The properties of the bulk have been measured in previous studies [1,8] and are summarized in Table 1. The materials were irradiated at room temperature with 74 MeV Kr ions at 5×10^{14} cm^{-2} fluence on the IRRSUD line of the GANIL facility (Caen, France). The samples were put on a water-cooled plate in order to minimize the sample heating under ion beam exposure. Following irradiation, samples were prepared for TEM by gluing the irradiated disks to polished safe disks. Then, they were sectioned, grinded down to a thickness of 100 μm, and finally ion beam thinned (Ion Slicer JEOL) with 6 kV Ar ions until perforation occurred near the interface. The specimens were cleaned using 2 kV Ar ions and then investigated using a conventional bright field and dark field imaging technique with a Philips CM30ST microscope. The Raman analyses are performed using a Labram HR (Jobin Yvon) micro spectrometer (λ = 632.8 nm, spectral resolution ≈ 2 cm^{-1}, lateral resolution ≈ 1 μm). A motorized micro-displacement stage (±0.1 μm) is used for the line scan measurement. Transverse section scanning is performed on irradiated materials.

3. Material characterization

To a first approximation, the initial damage has been estimated applying the Kinchin and Pease approximation [11] and the standard formulation of it by Norgett et al. [12] often referred to as 'NRT' model. Ion fluence were converted to their equivalent doses of displacement per atom (dpa) based on the SRIM 2003 full cascade simulation, with threshold displacement energies of 25 eV, for both Si and C [13]. The calculated damage according to the depth from the exposed surface is reported in Fig. 1. The IRRSUD line of the GANIL facility allows the observation of the combined electronic and nuclear interactions with matter, with typical ion energies in the 0.3–1 MeV $u.a^{-1}$ range. The dpa varies according to the depth and is higher in the nuclear cascade region, which corresponds to the region where incident ions mainly interact within the lattice via nuclear collision. Under neutron or ion irradiations, the disorder increases with the irradiation fluence to reach amor-

* Corresponding author. Address: LCTS, University of Bordeaux, 3 allée de la Boétie, 33600 Pessac, France.
E-mail address: cabrero@lcts.u-bordeauxl.fr (J. Cabrero).

0022-3115/$ - see front matter © 2009 Published by Elsevier B.V.
doi:10.1016/j.jnucmat.2009.11.006

Table 1
Properties and characteristics of irradiated and un-irradiated SiC sample (thermal properties at room temperature).

	SiC bulk	74 MeV Kr-interaction SiC, 5×10^{14} ions cm^{-2}	
		Electronic interaction area	Nuclear interaction area
Thermal conductivity (W m^{-1} K^{-1})	160 ± 20[8]	This study	This study
Density (kg m^{-3})	3200[1]	3200	2880[24]
Specific heat (J kg^{-1} K^{-1})	680[1]	680[1,23]	680[23]
Thickness (μm)	2000	8.6 ± 0.1 (TEM)	1 ± 0.1 (TEM)

phous state as soon as the fluence exceeds an amorphisation threshold. For crystalline 6H-SiC, this amorphisation threshold has been determined to be in the 0.2–0.6 dpa range at room temperature, depending on the nature of the particle and its energy [5,14–16]. With a fluence of 5×10^{14} ions cm^{-2}, we can expect an amorphisation of SiC in the nuclear interactions area. The dpa is smaller in the electronic interactions domain, between the surface and the nuclear cascade region; this region corresponds to the zone where ions slow down mainly by electronic energy loss processes. Several studies [17,18] demonstrate that SiC is not disordered by electronic interactions. It is also observed that heavy ion radiation can promote the recovery of displacement damage [19].

Bright field TEM and HRTEM observations of Kr 74 MeV irradiated SiC are reported in Fig. 2. Three zones are clearly distinguishable. The amorphous area is clearly observed in the nuclear interactions area, whereas a well ordered structure is observed in the electronic loss area: no damage is detected by TEM observation in this area. As the dpa number increases (as a function of depth, Fig. 1), HRTEM observations indicate that the lattice fringes are discontinuous and twisted because of the accumulation of irradiation-damages. In the peak damage region, which corresponds to the fully amorphous state under such irradiation, only a mottled contrast is observed. Raman scan of irradiated SiC are reported as a function of the depth in Fig. 3. The spectrum of the original material (depth = 11 μm) shows two main sharp and intense peaks at 788 cm^{-1} and 966 cm^{-1}, corresponding to the transverse optic (TO) and the longitudinal optic (LO) modes characteristic of crystalline SiC. In the electronic loss region (from the surface to about 7 μm), the intensity of the SiC peaks decreases, and their width increases with increasing dpa number (as the depth increases, see also Fig. 1). The evolution of the spectra indicates a moderate local

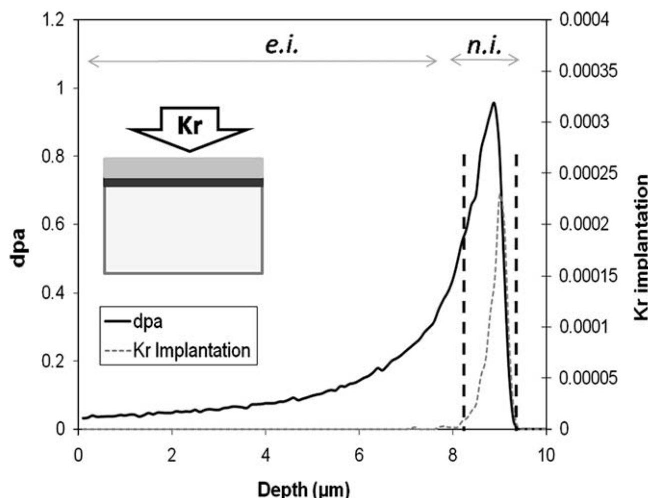

Fig. 1. SRIM estimation of damage in SiC implanted with 74 MeV Kr 5×10^{14} ions cm^{-2} (full line), and Kr implantation (dashed line). The borders of each domain are defined from TEM observations presented in Fig. 2. *e.i.*: electronic interactions, *n.i.*: nuclear interactions.

structure modification induced by irradiation. New peaks at 580 cm^{-1} and 850 cm^{-1} are detected and are associated to a distorted/disordered SiC structure corresponding to an intermediate state between amorphous and crystallized SiC, involving short range defects [20]. Dpa increase induces a decrease of both the crystalline peaks (700–1000 cm^{-1}) and disorder peaks intensities (580 cm^{-1}). In the nuclear zone (from 8.6 to 9.6 μm when dpa number is up to 0.5 dpa) the peaks at 580 cm^{-1} and 850 cm^{-1} vanish, and two broad bands appear slightly around 520 cm^{-1} and 1450 cm^{-1}. They are characteristic of Si–Si bonds (520 cm^{-1}) and C–C bonds (1450 cm^{-1}) and indicate that SiC is amorphous in this region [20]. It is obvious that such irradiations are responsible for a multi damaged layer. SiC is weakly damaged in the electronic loss region whereas it is totally amorphous in the nuclear cascade region. TEM and Raman analyses are in a good agreement.

4. Thermal conductivity measurement

The thermal conductivity of the two irradiated layers is measured using the modulated photothermal IR radiometry (MPTR) experiment [21]. It is based on amplitude and phase measurement of the thermal response to a periodic heat flux applied on the material surface (the same that has been irradiated). The photothermal excitation is generated from a single line laser (Ar^+, 514 nm, 2.5 W). The laser beam is modulated using an acousto-optic modulator from 1 kHz to 100 kHz. For those frequencies, the heat flux is unidirectional inside the investigated specimen. The infrared radiation emitted from the heated area is measured using a HgCdTe based photovoltaic infrared detector cooled down by liquid nitrogen. Since the temperature periodic variation at the heated area remains small (less than 10 K), it is assumed that the measured IR radiation is linearly proportional to this temperature. Heat transfer inside the sample is mathematically described from the heat diffusion equation and associated initial and boundary conditions [22]. According to the previous observations, the sample is thus viewed as a three layers material: the electronic interactions layer, the nuclear interactions layer and the un-irradiated SiC (Figs. 1 and 2). Although damage profiles in materials lead to expecting non linear thermal properties profiles versus the depth in the studied sample, thermal conductivity is assumed to be isotropic and homogeneous in each domain. The thicknesses of the electronic and nuclear interactions domains are very important parameters because they will have a great influence on the measured thermal conductivity of each layer. Thickness of the different layers was measured using TEM observation and is reported in Table 1. As the irradiated material is a graded damaged material (see Figs. 1–3), no contact thermal resistance between the different layers are taken into account. A sensitivity study shows that the amplitude and the phase are sensitive to the thermal conductivity of the two irradiated layers on two separable frequency domains (from 1 kHz to 3 kHz for the electronic interactions domain and from 3 kHz to 50 kHz for the nuclear interactions domain). It is therefore possible to estimate simultaneously the thermal conductivity of the two irradiated layers. Some values for the density and specific heat of amorphous SiC, have been presented in the litera-

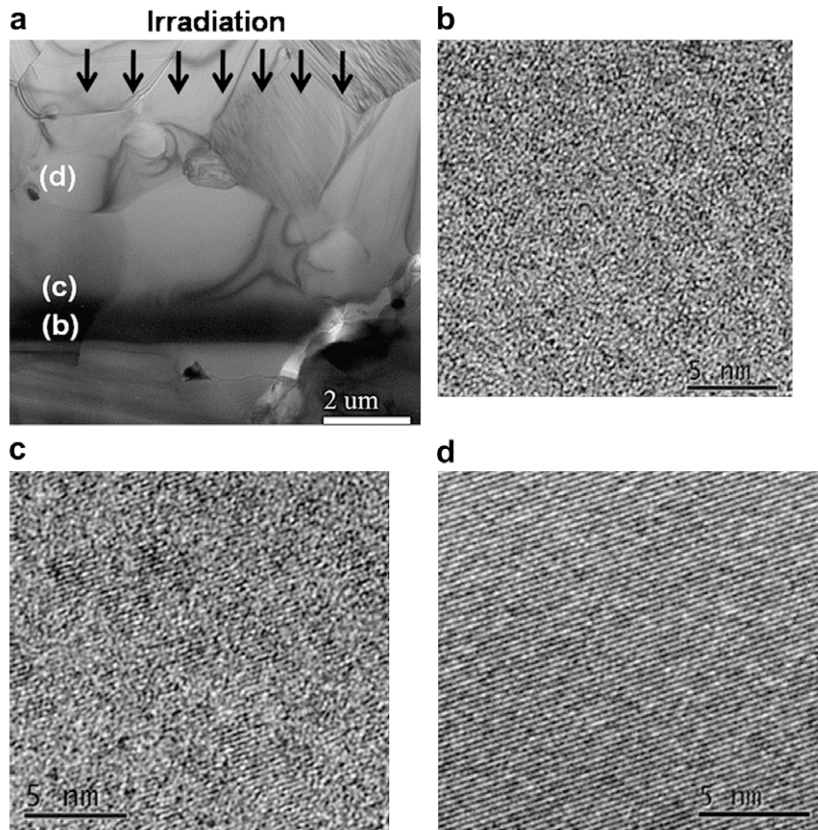

Fig. 2. Bright field TEM and HRTEM observations of Kr 74 MeV irradiated SiC, 5×10^{14} ions cm^{-2}. (a) Implanted layer, (b) Amorphous layer, (c) limit electronic interactions/nuclear interactions domain and (d) electronic interactions domain.

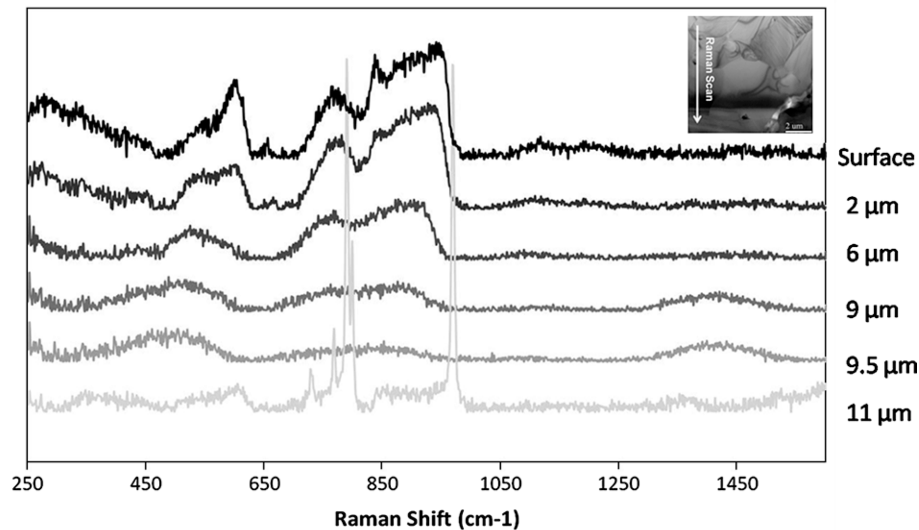

Fig. 3. Raman spectra of Kr 74 MeV, 5×10^{14} ions cm^{-2} irradiated SiC.

ture [1,23,24]. According to Lee et al. [23], the effect of irradiation on the specific heat of SiC is negligible. The specific heat of irradiated SiC is therefore assumed to be equal to specific heat of SiC (from room temperature to 1000 °C). The density remains unchanged in the area between the surface and the nuclear cascade region (the domain where ions slow down mainly by electronic energy loss process), but decreases in the nuclear cascade area. The variation is found to be about 1% (depending on the dose) if SiC remains crystallized, and about 10% if SiC becomes amorphous [24]. This density variation has been taken into account for both electronic and nuclear interactions domains.

Measurement of thermal conductivity of irradiated samples has been performed under secondary vacuum (10^{-5} m bar) from 200 °C to 1000 °C. Annealing of each sample was performed under

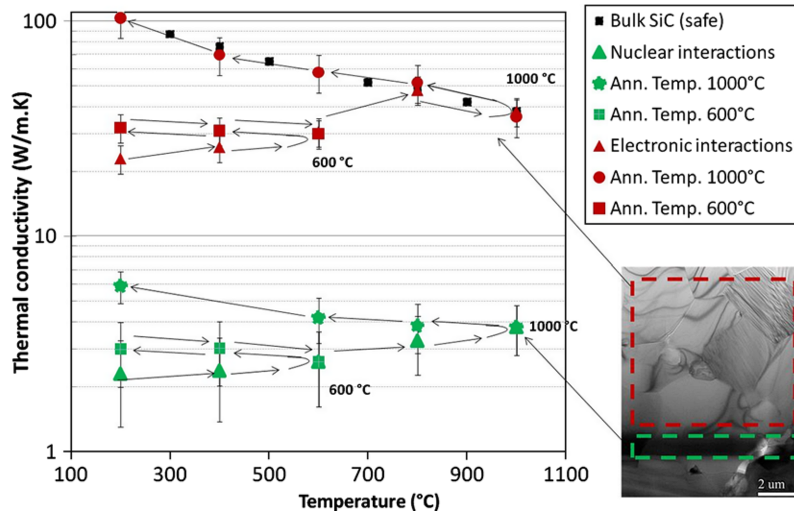

Fig. 4. Thermal conductivity as function of temperature, and annealing temperature (Ann. Temp.) for both electronic and nuclear interactions area.

high vacuum furnace for 20 min. Following each annealing step, the thermal conductivity was measured during cool down and is plotted as a function of temperature.

5. Results and discussion

Fig. 4 shows the variation of SiC thermal conductivity in both nuclear interactions ($k_{n.i.}$) area and electronic loss process area ($k_{e.i.}$) as a function of temperature and temperature annealing. First, thermal conductivity in the electronic interactions area is quite higher than thermal conductivity in the nuclear interactions. At 200 °C, $k_{n.i.}$ = 2.6 ± 1 W m^{-1} K^{-1} whereas $k_{e.i.}$ = 22 ± 5 W m^{-1} K^{-1}. This is in good agreement with Raman and TEM analysis. In the electronic interactions domain, thermal conductivity of as irradiated sample slightly increases with temperature from 200 °C to 600 °C. Above 600 °C, thermal conductivity increases more sharply and tends to reach thermal conductivity of non-irradiated SiC, indicating defects annealing process. From 800 °C, the contrast between the irradiated layer and the non-irradiated material is not very high: thermal conductivity is assumed to be equal to SiC bulk thermal conductivity. After annealing at 600 °C, $k_{e.i.}$ at 200 °C increased from 22 W m^{-1} K^{-1} to 32 W m^{-1} K^{-1}. No contrast is detected after annealing at 1000 °C which suggests a full restoration of the material in the electronic interactions area. After annealing at 600 °C and 1000 °C, the 1/k-data exhibit linear dependence with temperature (with A = 5.25 × 10^{-3} and B = 2.06 × 10^{-5} and R^2 = 0.94 after annealing at 1000 °C). Thus, thermal conductivity follows the classical law $k = \frac{1}{A+B\cdot T}$ which describes the thermal conductivity of lattice, according to temperature far after the Debye temperature. It is also noticed that this law takes into account the defect in the lattice. However, Raman analysis on the surface of the irradiated sample indicates that material is only partially restored (Fig. 5a): one of the two characteristic SiC peaks reappears at 788 cm^{-1}. The sensitivity of the MPTR may not be sufficient enough to measure thermal conductivity of a layer if its thermal conductivity is close to the thermal conductivity of the bulk material. Nevertheless, thermal conductivity in the electronic interactions area after annealing at 1000 °C seems to be very close from the thermal conductivity of the safe SiC.

The thermal conductivity in the nuclear interactions area is about 2.6 ± 1 W m^{-1} K^{-1} at 200 °C. Thermal conductivity of amorphous SiC is expected [10,24] to range from 3.6 to 5 W m^{-1} K^{-1} at room temperature, which is slightly higher than our measured values. The calculated minimal thermal conductivity for an amorphous SiC has been calculated [8] and is 3 W m^{-1} K^{-1}.

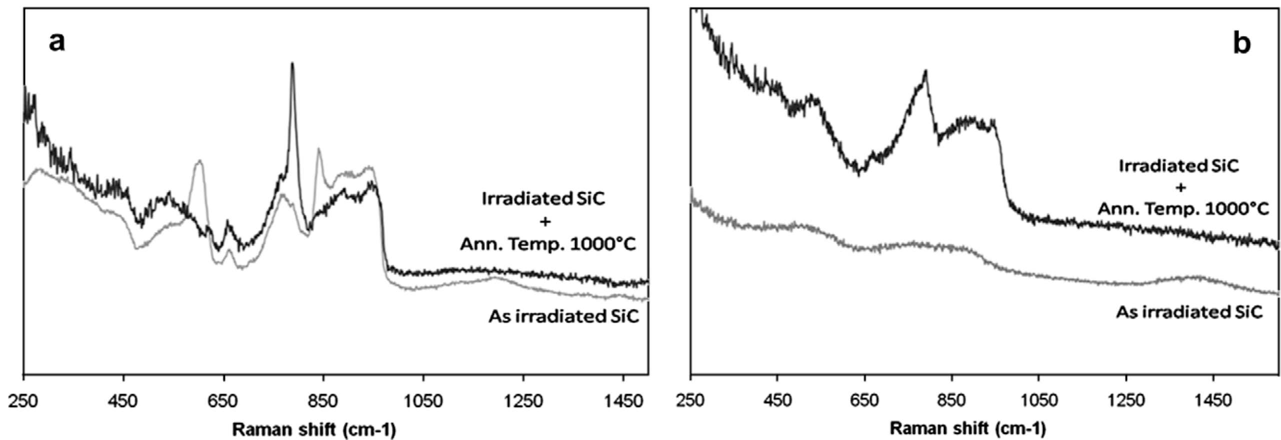

Fig. 5. Irradiated SiC Raman spectra on surface (a) and in the nuclear interactions domain (b), with thermal annealing (5 × 10^{14} ions cm^{-2} 74 MeV Kr).

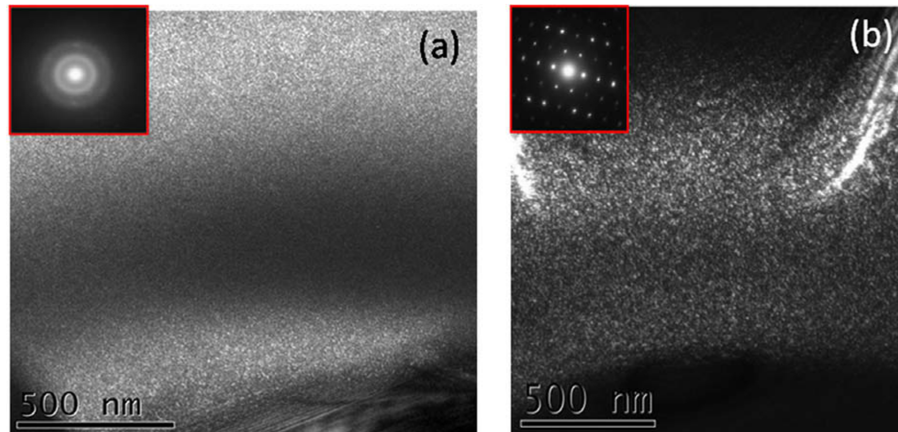

Fig. 6. Dark field TEM observations in the nuclear interactions domain. As irradiated (a) and 1000 °C annealing temperature (b).

Taking into account of the measurement error, our measured values are in a good agreement with the literature. After annealing at 600 °C, $k_{n.i.}$ at 200 °C is about 3 W m^{-1} K^{-1}, and 6 W m^{-1} K^{-1} after annealing at 1000 °C. Once irradiated SiC has been annealed, $k_{n.i.}$ decreases as function of temperature (very slight evolution, from 6 W m^{-1} K^{-1} at 200 °C to 3.8 W m^{-1} K^{-1} at 1000 °C), and the 1/k-data exhibit a linear dependence with the temperature (with $A = 0.153$, $B = 1.22 \times 10^{-4}$ and $R^2 = 0.93$ after annealing at 1000 °C). This suggests that umklapp scattering still occurs, even if the material is strongly damaged. After annealing at 1000 °C, the Raman bands at 520 cm^{-1} (Si–Si bonds) and 1420 cm^{-1} (C–C bonds) have disappeared, indicating that SiC is not any longer amorphous in the peak damage region (Fig. 5b), however SiC remains disordered. TEM observations confirm Raman analysis and photothermal radiometry experiments. In the peak damage region a partial recovery of initial microstructure is achieved by an annealing at 1000 °C. The SiC is not amorphous, but nanocrystallized (Fig. 6). HRTEM indicates that nano disordered domains are still present, and that epitaxial recrystallization occurs starting from the undamaged region towards the peak damage region. In the case of the amorphous material, the local perturbation in the strain field associated with distorted, or non-existent, bonds act as phonon-scattering centers. Clearly, increasing the short-range order in the SiC during annealing will reduce phonon-defect interactions and increase thermal conductivity. Those observations are in good agreement with other results whose reported temperature for onset of crystallization in amorphous SiC in the range of 800–1000 °C [4,16,24]. Thermal conductivity of as irradiated sample slightly increases with temperature indicating annealing of defects induced by irradiation. This is observed for both nuclear and electronic interactions domains, even if the increase is high for the last one. After annealing, thermal conductivity follow the law $k = \frac{1}{A+B \cdot T}$ indicating that thermal conductivity is controlled by both lattice vibration and defect due to irradiation.

6. Conclusions

SiC samples were irradiated with 74 MeV Kr ions with fluence of 5×10^{14} ions cm^{-2}. Raman and TEM analyses reveal that for this fluencies, SiC is amorphous in nuclear interaction domain (1 μm), and only weakly damaged in the electronic interactions domain. Thermal conductivity of the irradiated layer (few μm) is estimated using modulated photothermal IR radiometry experiment. The use of a three layers model (electronic loss area, nuclear interaction and un-irradiated material), enables the determination of thermal conductivity in the nuclear interaction area which is more representative of a neutron irradiation. Thermal conductivity increases with the temperature, indicating a partial annealing of defect. This is correlated to microstructure. After annealing at 1000 °C, thermal conductivity at 200 °C is 6 W m^{-1} K^{-1} and is 3.8 W m^{-1} K^{-1} at 1000 °C: 1/k-data exhibit a linear dependence with the temperature indicating that heat transfer is controlled by both lattice vibration and defect due to irradiation.

The advantage of such an approach is to avoid the limitations and difficulties generally encountered with neutron irradiation and it seems that the the modulated photothermal IR radiometry experiment is suitable for the characterization of irradiated materials. Other materials of interest for nuclear applications will irradiated, in the same conditions, but also with others ions, energies and temperatures. Thermal conductivity of those irradiated materials will be then measured in the range of 800–1000 °C and compared to irradiated SiC thermal conductivity.

Acknowledgment

The authors gratefully acknowledge the contributions of I. Monnet for her help during irradiation experiment and GNR MATINEX for its financial support.

References

[1] L.L. Snead, T. Nozawa, Y. Katoh, T.S. Byun, S. Kondo, D.A. Petti, J. Nucl. Mater. 371 (2007) 329.
[2] J.A. Edmond, S.P. Withrow, H.S. Kong, R.F. David, Mater. Res. Soc. Porc. 51 (1986) 395.
[3] X. Kerbiriou, J.M. Costantini, M. Sauzay, S. Sorieul, L. Thomé, J. Jagielski, J.J. Grob, J. Appl. Phys. 105 (2009) 073513.
[4] W.J. Weber, L.M. Wang, N. Yu, N.J. Hess, Mater. Sci. Eng. A 253 (1998) 62.
[5] L.L. Snead, S.J. Zinkle, Mater. Res. Soc. Proc. 373 (1995) 377.
[6] J. Grisola, B. de Mauduit, J. Gimbert, Th Billon, G. Ben Assayag, C. Bourgerette, A. Claverie, Nucl. Instr. Meth. Phys. Res. B 147 (1999) 62.
[7] L.L. Snead, S.J. Zinkle, J.C. Hay, M.C. Osborne, Instr. Meth. Phys. Res. B 141 (1998) 123–132.
[8] L. David, S. Gomes, G. Carlot, J.-P. Roger, D. Fournier, C. Valot, M. Raynaud, J. Phys. D: Appl. Phys. 41 (2008) 035502.
[9] S. Gomes, L. David, J.P. Roger, G. Carlot, D. Fournier, C. Valot, Eur. Phys. J.: Special Topics 153 (1) (2008) 87–90.
[10] J.P. Crocombette, G. Dumazer, N.Q. Hoang, J. Appl. Phys. 101 (2007) 023527.
[11] G.H. Kinchin, R.S. Pease, Rep. Prog. Phys. 18 (1955) 1.
[12] M.J. Norgett, M.T. Robinson, I.M. Torrens, Nucl. Eng. Des. 33 (1975) 50.
[13] R. Devanathan, W.J. Weber, J. Nucl. Mater. 278 (2000) 258.
[14] C.J.Mc. Hargue, J.M. Williams, Nucl. Instr. Meth. Phys. Res. 80 (1993) 889.
[15] A. Audren, I. Monnet, Y. Leconte, X. Portier, L. Thomé, M. Levalois, N. Herlin-Boime, C. Reynaud, Nucl. Instr. Meth. Phys. Res. B 266 (12–13) (2008) 2806–2809.
[16] E. Wendler, A. Heft, W. Wesch, Nucl. Instr. Meth. Phys. Res. B 141 (1998) 105–117.
[17] A. Benyagoub, Nucl. Instr. Meth. Phys. Res. B 266 (2008) 2766.

[18] A. Audren, A. Benyagoub, L. Thomé, F. Garrido, Nucl. Instr. Meth. Phys. Res. B 266 (2008) 2810.
[19] S.J. Zinkle, V.A. Skuratov, D.T. Hoelzer, Nucl. Instr. Meth. Phys. Res. B 191 (2002) 758.
[20] S. Sorieul, J.-M. Costantini, L. Gosmain, L. Thomé, J.-J. Grob, J. Phys. Condens. Mater 18 (2006) 5235.
[21] J.L. Battaglia, A. Kusiak, M. Bamford, J.C. Batsale, Int. J. Therm. Sci. 45 (2006) 1035.
[22] J.-L. Battaglia, A. Kusiak, Int. J. Thermophys. 28 (2007) 1563.
[23] C.W. Lee, J.F. Pineau, J.C. Corelli, J. Nucl. Mater. 108 (1982) 678.
[24] L.L. Snead, S.J. Zinkle, Nucl. Instr. Meth. Phys. Res. B 191 (2002) 497.